ACS BIO & MED CHEM Au
AN OPEN ACCESS JOURNAL OF THE AMERICAN CHEMICAL SOCIETY

pubs.acs.org/biomedchemau
Article

Enhanced Sequence-Specific DNA Recognition Using Oligodeoxynucleotide-Benzimidazole Conjugates

Souvik Sur, Suresh Pujari, Nihar Ranjan, Lidivine Azankia Temgoua, Sarah L. Wicks, Andrea Conner, and Dev P. Arya*

Cite This: ACS Bio Med Chem Au 2024, 4, 154−164
Read Online

ABSTRACT: Synthetic modification of oligodeoxynucleotides (ODNs) via conjugation to nucleic acid binding small molecules can improve hybridization and pharmacokinetic properties. In the present study, five Hoechst 33258 derived benzimidazoles were conjugated to T rich ODNs and their hybridization effectiveness was tested. Thermal denaturation studies revealed significant stabilization of complementary duplexes by ODN-benzimidazole conjugates, with the extent of stabilization being highly dependent on the length of the linker between DNA and benzimidazole. The increases in thermal stability were determined to be due to the binding of the benzimidazole moiety to the duplex. Circular dichroism and molecular modeling studies provided insights toward the influence of conjugation on duplex structure and how linker length impacts placement of the benzimidazole moiety in the minor groove. Furthermore, thermal denaturation studies with the complementary strand containing a single base mismatch or being RNA revealed that covalent conjugation of benzimidazoles to an ODN also enhances the sequence specificity. The fundamental studies reported herein provide a strategy to improve the stability and specificity properties of the ODN probes, which can be of use for targeting and diagnostics applications.

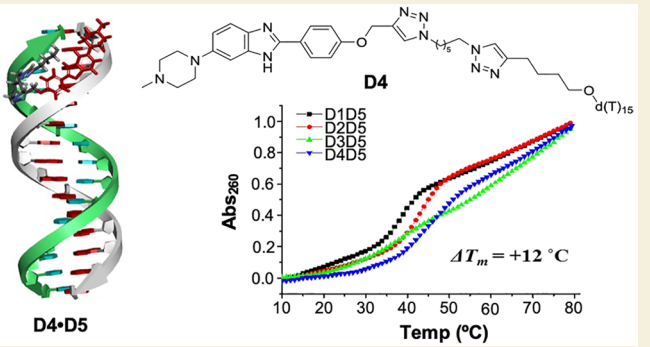

KEYWORDS: *molecular recognition, AT minor groove binder, bioconjugation, click chemistry, thermal denaturation, circular dichroism, molecular modeling*

INTRODUCTION

Oligodeoxynucleotide (ODN) based probes are valuable tools for studying molecular recognition of nucleic acids and investigating biological processes. Short ODNs (<25 bases long) bind in a sequence-specific manner to complementary single stranded (ss) DNA and RNA. This complementarity has been utilized to manipulate cellular processes such as transcription and translation.[1−3] Additionally, the use of short ODNs has opened new avenues of therapeutic development with there being currently 18 FDA approved ODN based therapeutics for treatment of various diseases.[4]

Synthetic modification of short ODNs via conjugation to nucleic acid binding small molecules can improve the hybridization and pharmacokinetic properties. Upon hybridization to a complementary sequence, a small molecule can bind and stabilize the DNA duplex or DNA•RNA hybrid. As a result, ODN-small molecule conjugates can have enhanced sequence specificity and potency relative to their unconjugated counterparts.[5−7] ODN-small molecule conjugates have been used in widespread applications as sensing and diagnostic probes,[8−10] cellular targeting agents,[11] and therapeutics.[12,13]

Hoechst dyes are a class of nucleic acid binding fluorophores. These dyes are known to tightly bind the minor groove of B-form DNA duplexes preferentially at A/T-rich stretches.[14−16] The core structure of Hoechst dyes, such as Hoechst 33258, is a bis-benzimidazole. The benzimidazole moieties form hydrogen bonding contacts to thymine O2-carbonyls and adenine N3-nitrogens, providing sequence specific recognition.[17,18] Additionally, the fluorescence properties of the benzimidazole moiety, which is enhanced upon binding nucleic acids, can be used as a reporter for DNA-binding.[5,19] Compared to bis-benzimidazoles, monobenzimidazole derivatives have also been reported as fluorescent DNA minor groove binders but are less challenging to synthesize.[20−24] Conjugation of monobenzimidazole derivatives to DNA is expected to provide fluorescent hybridization probes that have enhanced sequence specificity and stability properties as compared to unconjugated DNA. Furthermore, an evaluation of the hybridization properties of DNA-benzimida-

Received: November 23, 2023
Revised: March 28, 2024
Accepted: March 28, 2024
Published: April 16, 2024

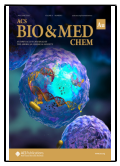

https://doi.org/10.1021/acsbiomedchemau.3c00074
ACS Bio Med Chem Au 2024, 4, 154−164

Scheme 1. Synthesis of dT_{15}-Benzimidazole Conjugates

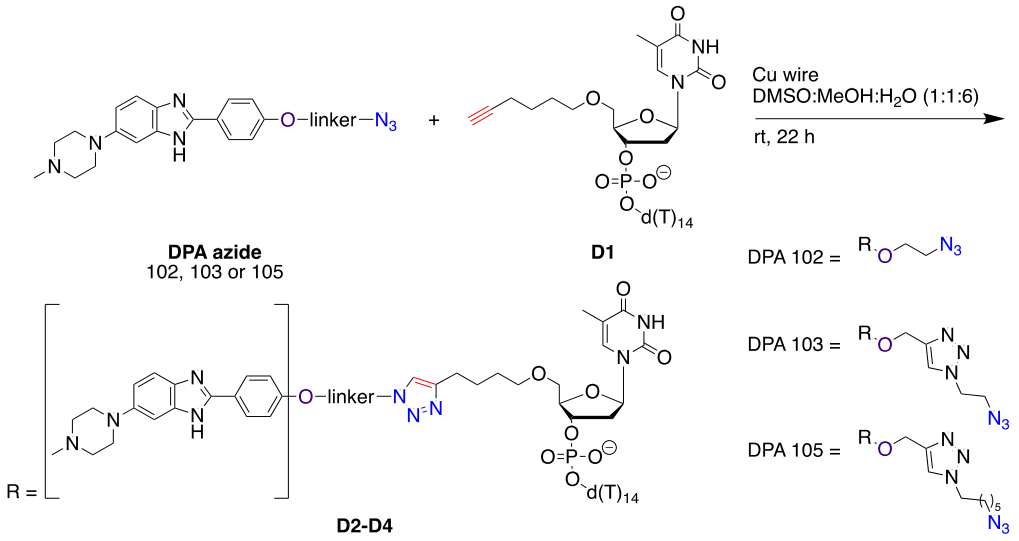

zole conjugates will inform on the generality of our approach and the utility of these probes for in vitro studies.

RESULTS AND DISCUSSION

Conjugation of Benzimidazole Derivatives to ssDNA Is General and Efficient

The compounds DPA 102, DPA 103, and DPA 105 are derived from Hoechst 33258 (Scheme 1). They are composed of the same subunits as Hoechst 33258 except that they are monobenzimidazoles (referred to as benzimidazoles henceforth) instead of bis-benzimidazoles. Additionally, the derivatives are functionalized with azide linkers of varying lengths. The linker length between the phenol ether of Hoechst 33258 derivatives and the azide unit varies from 2 atoms (DPA 102) and 6 atoms (DPA 103) to 10 atoms (DPA 105).

Given the AT-rich binding preferences of benzimidazoles, we chose to conjugate the compounds to a commercially available dT_{15} ssDNA that has an alkyne modification at the 5′-end. The synthesis of ODN-benzimidazole conjugates was achieved using click chemistry.[25,26] The dT_{15} ssDNA (D1, containing the alkyne unit) and the benzimidazoles (containing the complementary azide units) were used as the starting materials (Scheme 1). Alkynes and azides were reacted in the presence of a copper wire catalyst to form corresponding DNA-benzimidazole conjugates (D2-D4). Initial HPLC analysis showed that the desired products were obtained in >90% purity (Figures S1−S3). These conjugates were then purified by reversed phase HPLC and fractions for each conjugate were collected and pooled to afford pure samples that were further used for spectroscopic studies. The characterization of the synthesized conjugates was performed by MALDI-TOF mass spectrometry, UPLC-MS and UV−vis spectroscopy, which corroborated the incorporation of the benzimidazole unit (Figures S4−S12).

The DNA-benzimidazole conjugates D1-DPA 102 (D2), D1-DPA 103 (D3), and D1-DPA 105 (D4) were then evaluated for their hybridization to ssDNA and ssRNA (Table 1). The relative stabilities of these duplexes were evaluated by thermal denaturation and monitoring by both UV−vis and fluorescence spectroscopy. We chose complementary ssDNA (D5) as well as ssRNA (R1) to study the hybridization of the ODN-benzimidazole conjugates to both target nucleic acids. Three mismatched ssDNA sequences (D6, D7 and D8) and ssRNA sequences (R2, R3 and R4) were also studied to observe the effects of mismatches on the recognition by these conjugates.

Table 1. 15 mer Homo-Oligomer and Mismatch Sequences Used in this Study[a]

Sequence	Code
5′-HexynyldT_{15}	D1
5′-dT_{15}	D1B
5′-HexynyldT_{15}-DPA102	D2
5′-HexynyldT_{15}-DPA103	D3
5′-HexynyldT_{15}-DPA105	D4
5′-dA_{15}	D5
5′-d(AAA AAA AGA AAA AAA)	D6[a]
5′-d(AAA AAA AAA AAA AGA)	D7[a]
5′-d(AGA AAA AAA AAA AAA)	D8[a]
5′-rA_{15}	R1
5′-r(AAA AAA AGA AAA AAA)	R2[a]
5′-r(AAA AAA AAA AAA AGA)	R3[a]
5′-r(AGA AAA AAA AAA AAA)	R4[a]

[a]Sequences D6 & R2, D7 & R3, and D8 & R4 are mismatch sequences with one base "G" in the eighth, 14th, and second position from 5′ end, respectively.

Linker Length Plays a Critical Role in Ligand Binding to the DNA Duplex

The thermal melting temperatures (T_ms) determined by UV spectroscopy are listed in Table 2. The T_m for the control

https://doi.org/10.1021/acsbiomedchemau.3c00074
ACS Bio Med Chem Au 2024, 4, 154−164

Table 2. UV Thermal Denaturation of Different T15 DNA•DNA Duplexes

duplex	control	T_m (°C)[a]	ΔT_m (°C)[a]	$\Delta\Delta T_m$ (°C)
D1B•D5	NA	39.6	NA	NA
D1•D5	NA	36.5	NA	NA
D2•D5	D1•D5	44.0	+7.5	NA
D3•D5	D1•D5	45.0	+8.5	NA
D4•D5	D1•D5	48.5	+12.0	NA
D1•D6	D1•D5	34.8	−1.7	NA
D4•D6	D4•D5	38.1	−10.4	−8.7
D1•D7	D1•D5	35.8	−0.7	NA
D4•D7	D4•D5	34.2	−14.3	−13.6
D1•D8	D1•D5	35.2	−1.3	NA
D4•D8	D4•D5	37.3	−11.2	−9.9
D1•D5 + DPA 102[b]	D1•D5	38.1	+1.6	NA
D1•D5 + DPA 103[b]	D1•D5	40.3	+3.8	NA
D1•D5 + DPA 105[b]	D1•D5	41.8	+5.3	NA

[a]All data in this table are derived from UV melting experiments, and values are the average of at least two determinations (± 1.0 C). [b]Concentration of unconjugated benzimidazole is 2 μM

dT_{15}•dA_{15} (D1•D5) DNA duplex was 36.5 °C in the presence of 100 mM NaCl. Benzimidazole modified ODN conjugates D2, D3, and D4 afforded 7.5, 8.5, and 12.0 °C higher thermal stabilization, respectively, when hybridized with D5 as compared to the D1•D5 control (Figure 1A). These results shed light on two important outcomes: (i) the ODN-benzimidazole conjugates D2, D3, and D4 stabilize DNA duplexes much better than their unmodified counterpart under identical salt and buffer concentrations and (ii) the stabilization of DNA duplexes by ODN conjugates is dependent on the linker spacing between the 5′-end of the ODNs and of the benzimidazoles. As the linker length increases from 9 (D2) to 17 (D4) atoms, the thermal stabilization of the DNA duplexes increased from 7.5 to 12 °C. For control experiments in which the DNA duplex (D1•D5) was denatured in the presence of unconjugated benzimidazoles (DPA 102, DPA 103, and DPA 105), the increase in thermal stabilization was much lower (1.6 to 5.3 °C) (Figure 1B). These results clearly show that covalent conjugation of benzimidazoles to the ODN leads to stronger stabilization of the DNA duplex than the unconjugated control.

Since the benzimidazole moiety is fluorescent, T_ms for the DNA duplexes were also determined by fluorescence spectroscopy. The fluorescence of the benzimidazole moiety increases upon binding to nucleic acids.[5] Therefore, a gradual decrease in fluorescence while heating a preformed duplex would be indicative of the benzimidazole moiety disassociating from the duplex. The fluorescence of preformed DNA duplexes was monitored as the temperature was increased from 20 to 90 °C at 10 °C intervals (Figure 2). In all cases, a gradual decrease in the fluorescence intensity was observed (Figures S13−S15). This result implies that the benzimidazole moiety of each conjugate binds to the DNA duplex, leading to increased thermal stability. From fluorescence melting experiments, the T_ms of D2•D5, D3•D5, and D4•D5 were determined to be 49.0, 48.9, and 54.8 °C, respectively. These T_ms are similar to those that were found by using UV spectroscopy (Table 2). Thus, from both melting experiments, the ODN-benzimidazole conjugate D4 was found to form the most stable duplex among the three.

Benzimidazole Conjugation Makes the DNA Recognition Highly Sequence-Specific

Three complementary sequences containing a single base mismatch were then chosen to evaluate their effect on the thermal stabilization of the duplexes by the ODN-benzimidazole conjugates. An adenine was replaced with a guanine in D5 to yield three different sequences (D6, D7, and D8) (Table 1). We chose the ODN-benzimidazole conjugate D4 for studies with mismatched sequences, as it was found to be most effective in DNA duplex stabilization with the complementary ODN D5. All of the unconjugated mismatched DNA duplexes (D1•D6, D1•D7, and D1•D8) showed minor instability (∼1−2 °C) as compared to the complementary D1•D5 control (Table 2). In stark comparison, significant destabilization was seen in the case of benzimidazole conjugated mismatched DNA duplexes (D4•D6, D4•D7, and D4•D8) when compared to control D4•D5 (Figure 3A) (Table 2). The largest destabilization was observed with duplex D4•D7 (−14.3 °C). In D7, the A to G mismatch is most toward the 3′ end (position 14). In D4, the benzimidazole is conjugated to the 5′-end and thus interacts with the nearby duplex region. Therefore, the stability of D4•D7 is most significantly affected as a result of the mismatch site in D7 being the nearest to the

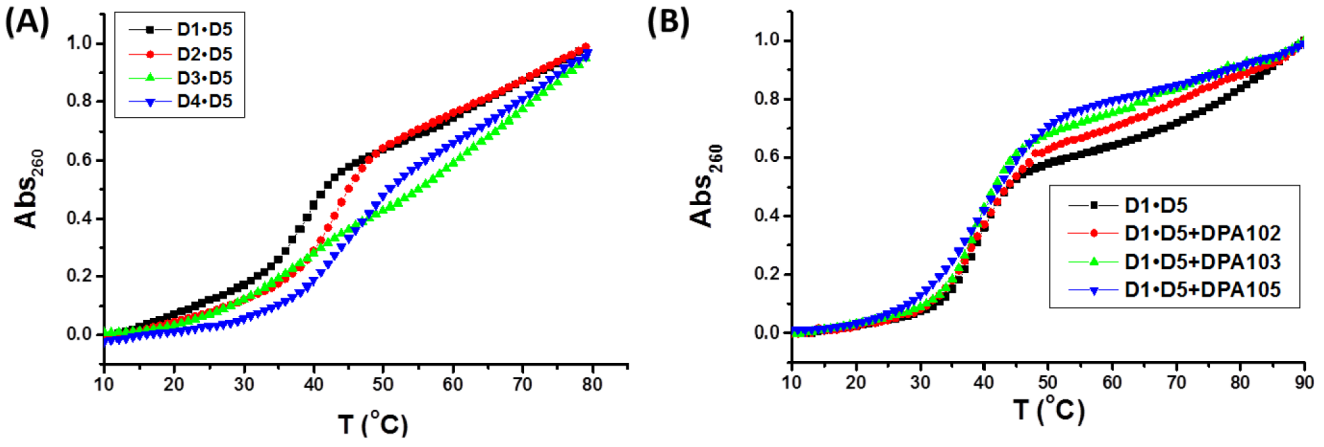

Figure 1. UV thermal denaturation profiles of DNA duplexes. (A) Thermal denaturation profiles of DNA duplexes (2 μM); (B) thermal denaturation profiles of D1•D5 (2 μM) in the absence and presence of 2 μM DPA 102, DPA 103, and DPA 105. Buffer was 10 mM sodium cacodylate, 0.5 mM EDTA, and 100 mM NaCl at pH = 7.0. The heating was done at a rate of 0.25 °C/min.

https://doi.org/10.1021/acsbiomedchemau.3c00074
ACS Bio Med Chem Au 2024, 4, 154−164

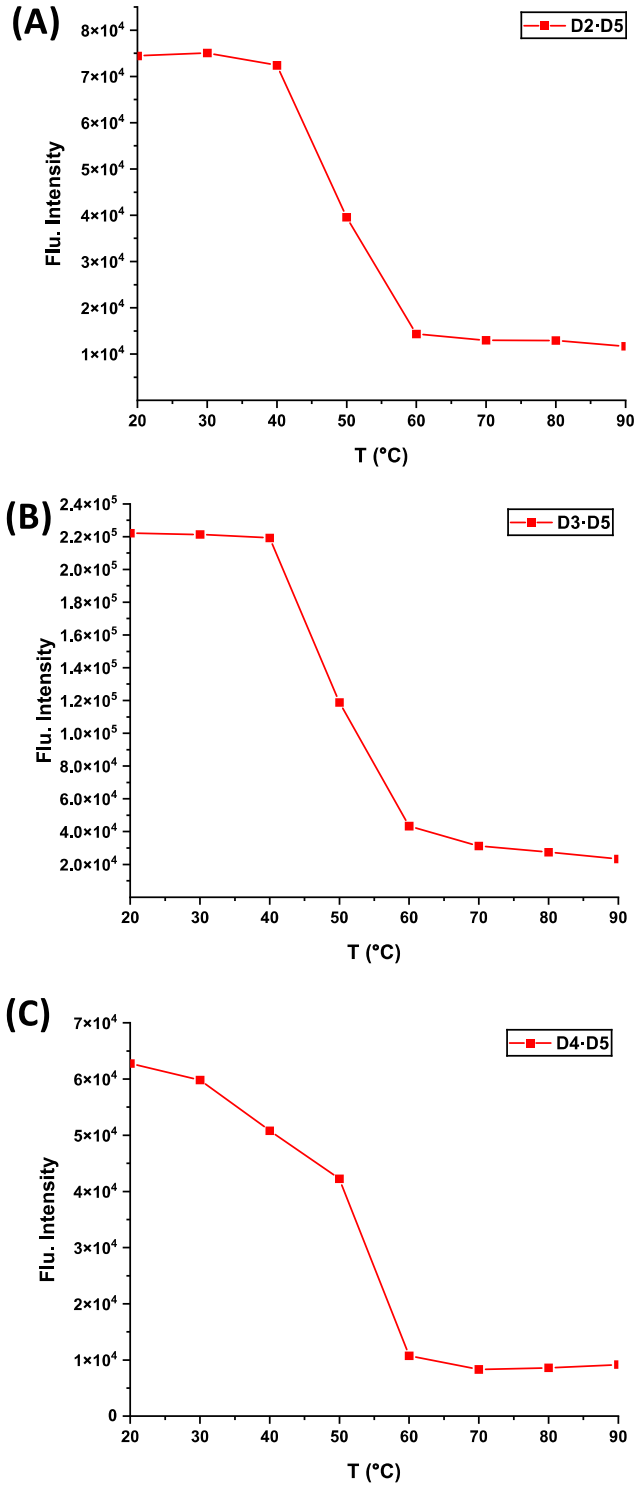

Figure 2. Fluorescence thermal denaturation profiles of DNA duplexes. (A) D2●D5; (B) D3●D5; and (C) D4●D5.

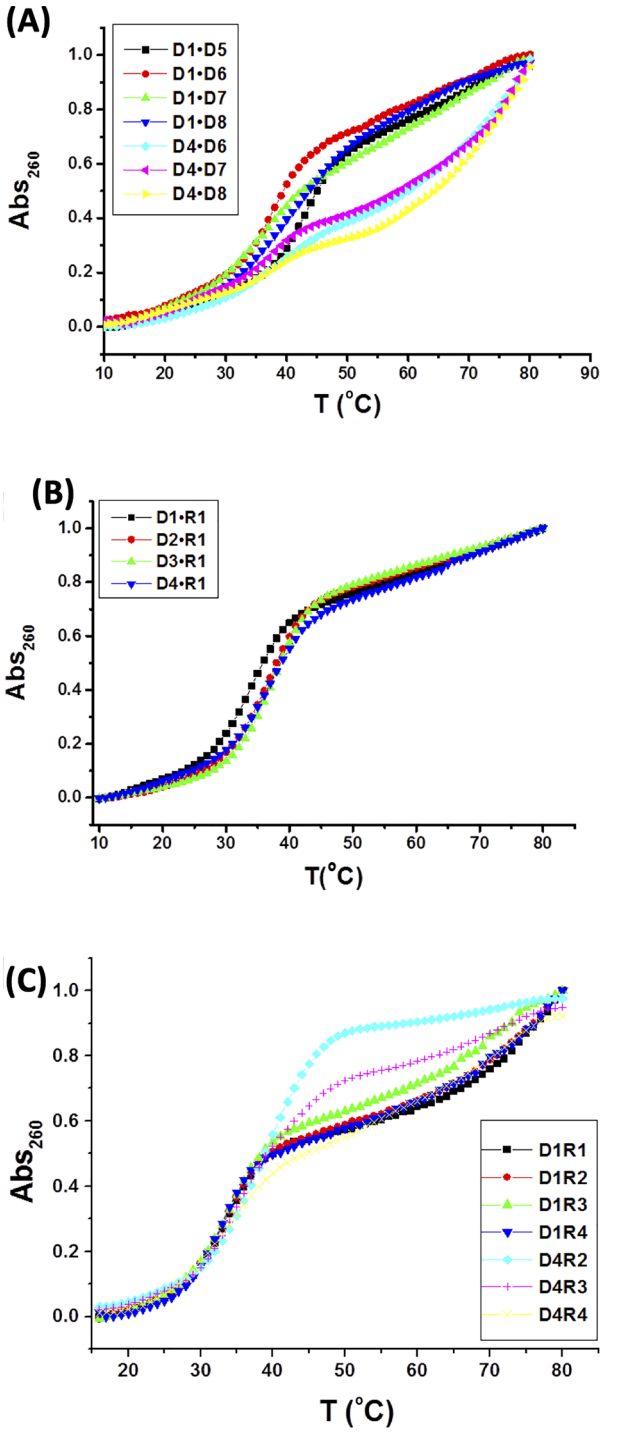

Figure 3. UV melting profiles of mismatch DNA duplexes, DNA●RNA hybrids, and mismatch DNA●RNA hybrids. (A) thermal denaturation profiles of A to G mismatch DNA duplexes; (B) thermal denaturation profiles of DNA●RNA hybrids; (C) thermal denaturation profiles of A to G mismatch DNA●RNA hybrids.

conjugation site in D4. Significant destabilization was also observed when the A to G mismatch occurred in the middle of the complementary sequence (D6, position 8, −10.4 °C) but to a lesser extent, as would be expected given that the mismatch is farther from the conjugation site. These results suggest that covalent conjugation of benzimidazoles to the ODN enhances its sequence specificity, as evidenced by the larger decrease in thermal stability of DNA duplexes.

The Native AT Rich Duplex Shows Little Change in Thermal Stability with a Single Mismatch

While there is no doubt that the benzimidazole moiety helps confer an added level of sequence specificity to the AT rich DNA duplex, what is intriguing is the little change in T_m observed when the benzimidazole is absent from mismatched duplexes (D1●D6, D1●D7, and D1●D8). Melting tools online predict that an A to G mismatch in the target sequence should

https://doi.org/10.1021/acsbiomedchemau.3c00074
ACS Bio Med Chem Au 2024, 4, 154−164

lead to an 8−10 °C decrease in T_m.[27,28] Previous work by McLaughlin has also shown that a mixed AT rich DNA duplex shows an ∼8 °C drop in T_m when a single A to G mismatch is introduced.[29] To our surprise, we saw a negligent change in T_m (∼1−2 °C). There are, however, two differences from previous work that should be noted. One, our sequence is a homooligomer duplex, as opposed to a mixed sequence containing G and C bases. Second, our DNA control (D1) contains a hexynyl linker that was used to conjugate the benzimidazole.

We therefore repeated our melting experiments with a dT_{15} homoligomer that does not contain the hexynyl linker (D1B) (Table 1). The mismatched duplexes, without the hexynyl linker (D1B•D6, D1B•D7 and D1B•D8), have T_ms that are 3−5 °C lower than the AT rich control (D1B•D5) (Table S1). The data suggest that the hexynyl linker has an effect on the structure of the duplex that allows it to accommodate a mismatch better than the native ssDNA. To further confirm our findings, we compared our results that used ODNs purchased from IDT to those obtained from Sigma-Aldrich (Figures S16−S18). In both cases, we found that the presence of the hexynyl linker has a similar effect on the duplex such that incorporating a mismatch does not lower the T_m significantly, contrary to the predicted result (Table S1). These findings raise intriguing questions about linker identity and its effect on the hybridization properties of mismatched duplexes. In particular, it is of interest to assess the individual contributions of the benzimidazole moiety and triazole linker to the overall decrease in thermal stability observed for mismatched duplexes. Further biophysical and structural studies that thoroughly investigate different linkers, such as the triazole linker, and their impact on thermal stability of mismatched duplexes will provide valuable insights into the effects these modifications may have on DNA structure but are outside the scope of this present work.

Benzimidazole Conjugation Stabilizes the DNA•DNA Duplex Much More Effectively Compared to the RNA•DNA Hybrid

We then tested the thermal stabilization of these ODN-benzimidazole conjugates on DNA•RNA hybrids by hybridizing D2, D3, and D4 with complementary ssRNA (R1) (Table 1). UV spectroscopy determined T_ms for hybrids D2•R1, D3•R1, and D4•R1 were 3.0, 1.7, and 2.7 °C higher, respectively than those for the control (D1•R1, T_m = 35.1 °C) (Figure 3B). From fluorescence melting experiments, the T_ms of D2•R1, D3•R1, and D4•R1 were determined to be 46.0, 41.6, and 39.0 °C, respectively (Figures S19−S22). These T_ms are similar to those that were found using UV spectroscopy (Table 2). Control experiments were also conducted in which the DNA•RNA hybrid D1•R1 was denatured in the presence of unconjugated benzimidazoles (DPA 102, DPA 103, and DPA 105). The addition of unconjugated benzimidazoles increased thermal stabilization of D1•R1 by ∼2−3 °C which is similar to the T_m change observed with the covalently attached ODN-benzimidazoles (Table 3). While these results show the ability of the conjugates of the ODN-benzimidazole to bind and stabilize DNA•RNA hybrids, it is discernible that the thermal stabilization is much lower compared to DNA duplexes and is not enhanced by conjugation. The differences in thermal stabilization of DNA•RNA hybrids and DNA duplexes by ODN-benzimidazole conjugates are likely to be caused by the different shapes adopted by the nucleic acid structures and the differential binding of benzimidazoles, which are known to preferentially bind to AT rich B-form structures than A-form structures like dsRNA.[30−32]

Table 3. UV Thermal Denaturation of Different T_{15} DNA•RNA Hybrids

hybrid	control	T_m (°C)[a]	ΔT_m (°C)[a]	$\Delta\Delta T_m$ (°C)
D1•R1	NA	35.1	NA	NA
D2•R1	D1•R1	38.1	+3.0	NA
D3•R1	D1•R1	36.8	+1.7	NA
D4•R1	D1•R1	37.8	+2.7	NA
D1•R2	D1•R1	34.8	−0.3	NA
D4•R2	D4•R1	36.3	−1.5	−1.2
D1•R3	D1•R1	34.3	−0.8	NA
D4•R3	D4•R1	34.7	−3.1	−2.3
D1•R4	D1•R1	34.1	−1.0	NA
D4•R4	D4•R1	35.9	−1.9	−0.9
D1•R1 + DPA 102[b]	D1•R1	38.2	+3.1	NA
D1•R1 + DPA 103[b]	D1•R1	37.8	+2.7	NA
D1•R1 + DPA 105[b]	D1•R1	37.2	+2.1	NA

[a]All data in this table are derived from UV melting experiments, and values are the average of at least two determinations (± 1.0 C). [b]Concentration of unconjugated benzimidazole is 2 μM.

Similarly, we also performed melting experiments with three A to G mismatch RNA sequences (R2, R3, and R4) (Table 1). All of the nonbenzimidazole conjugated mismatched DNA•RNA hybrids (D1•R2, D1•R3, and D1•R4) showed minor instability (∼1 °C) as compared to the complementary D1•R1 control (Table 3). Hybridization of ODN-benzimidazole conjugate D4 to mismatch RNA sequences moderately destabilized hybrids compared to control D4•R1 (Figure 3C). Melting temperatures decreased by −1.5, −3.1, and −1.9 °C for D4•R2, D4•R3, and D4•R4, respectively (Table 3). These results show the ability of ODN-benzimidazole conjugates to destabilize mismatched DNA•RNA hybrids, albeit to a lesser extent than mismatched DNA duplexes and to varying degrees depending on the position of the mismatched base.

CD Spectroscopy Studies Confirm a B-Form DNA•DNA Duplex

The impact of ODN-benzimidazole conjugates on the secondary structure of DNA duplexes and DNA•RNA hybrids was evaluated using circular dichroism (CD) spectroscopy. The preformed DNA duplex control D1•D5 showed a negative peak at ∼245 nm and a positive peak at ∼280 nm along with a shoulder at 225 nm, reflecting a typical B-form structure as would be expected with this duplex (Figure S23A).[33] The CD plots for duplexes formed with the ODN-benzimidazole conjugates (D2•D5, D3•D5, and D4•D5) were also characteristic of a B-form structure. In the same manner, we recorded CD plots of ssRNA R1 hybridized to complementary DNA D1 and ODN-benzimidazole conjugates. The CD spectra of these DNA•RNA hybrids (D1•R1, D2•R1, D3•R1, and D4•R1) all showed a negative peak at ∼245 nm and a broad positive signal with maxima at 260 and 280 nm (Figure S23B). The CD profiles are typical of an intermediate structure between A- and B-forms as observed with DNA•RNA hybrids.[33] Thus, our conformational studies revealed that ODN-benzimidazole conjugates do not significantly alter the nucleic acid secondary structure upon binding ssDNA and ssRNA.

https://doi.org/10.1021/acsbiomedchemau.3c00074
ACS Bio Med Chem Au 2024, 4, 154−164

Modeling Studies Highlight the Role of the Linker in Allowing the Benzimidazole Unit to Dock into the DNA Duplex Groove

To better understand the experimental results, molecular modeling studies were performed on ODN-benzimidazole conjugates D2, D3, and D4. Molecular docking followed by energy minimization was carried out with these conjugates. Taking noncovalently bonded complexes as controls, we can easily compare the difference in the stability increment upon conjugation. Molecular docking of DPA 102, 103, and 105 to the unconjugated DNA duplex (D1•D5) showed minor groove binding in all three cases (Figure S24). The docking score was found to be most optimum with DPA 105 (−13.78 kcal/mol), whereas with DPA 102 and DPA 103 moderate scores of −8.32 and −10.73 kcal/mol were obtained, respectively (Table S2).

Covalently attached ODN-benzimidazole DNA complexes had better stabilization energy compared to the unconjugated DNA duplex and noncovalently bonded complexes. Here we found the most stable system to be D4•D5 (conjugated with DPA 105) with an energy of −5166.60 ± 14.54 kcal/mol compared with D2•D5 and D3•D5, which showed higher energies of −5004.42 ± 21.41 and −5032.64 ± 10.86 kcal/mol, respectively (Table S2). Overall, the covalent conjugation of benzimidazole to ssDNA (such as D1) increases the stability of all three complexes (D2•D5, D3•D5 and D4•D5) in comparison with D1•D5.

From the above observations, it is evident that D4•D5 forms a more stable DNA duplex than D2•D5 and D3•D5. The thermal melting experiments with D4•D5 showed extra stability of 4.5 °C over D2•D5 and 3.5 °C over D3•D5, where the linker length clearly affects the binding. Analysis of the energy minimized structure of the D4•D5 duplex revealed that the longer linker enables the benzimidazole moiety to bend and accommodate itself in the minor groove of the duplex, explaining its most efficient thermal stabilization among the three duplexes (Figure 4). By comparing energy minimized structures of D4•D5 and D3•D5 complexes, we can conclude that the extra four methylene groups in DPA 105 plays a vital role in the duplex stability. The increased linker length in DPA 105 helps the benzimdaizole to effectively bind in the minor groove of D4•D5 upon covalent conjugation, whereas the benzimidazole moiety is not optimally placed in the minor groove of the D3•D5 complex (Figure S25).

Stabilization of a 12 Base Pair Mixed Base DNA Duplex by the ODN-Benzimidazole Conjugate Reveals Further Considerations for Linker Design

Given the improved stabilization and sequence recognition of homooligomer D1 by conjugation to benzimidazole derivatives, we wanted to see if our approach could be extended to additional DNA sequences such as hetero-oligomers. We chose a dT_6 oligomer that is flanked by three G/C bases (D9, Table 4). The shortened AT-rich stretch should still provide a binding site for benzimidazole derivatives, although the linker length may need to be changed to optimize recognition. Therefore, we synthesized two additional benzimidazole derivatives: DPA 104 and DPA 6011 (Schemes S1 and S2) (Figures S26−S48). The linker length of DPA 104 is 9 atoms, falling in between the two best dT_{15}:dA_{15} stabilizers DPA 103 (6 atoms) and DPA 105 (10 atoms). For DPA 6011, the linker length was extended to 12 atoms. By testing both DPA 104 and DPA 6011, we will gain insight toward the generality of our approach and considerations for linker design.

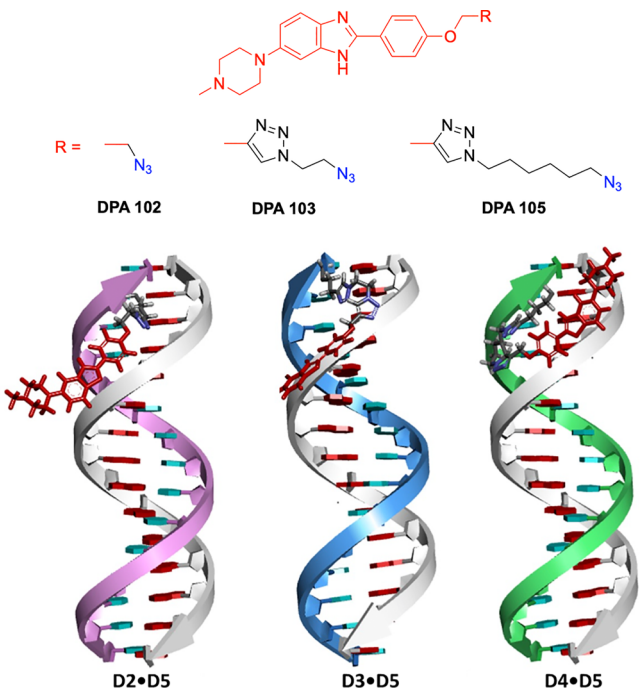

Figure 4. Energy minimized structures of D2•D5, D3•D5, and D4•D5. The common part "R" is represented in red and the different linkers are in characteristic colors. Conjugated thymine rich ssDNAs are colored purple (D2), blue (D3), and green (D4), whereas the complementary adenine rich ssDNA is colored gray.

We conjugated DPA 104 and DPA 6011 to D9 and obtained pure conjugates to use for spectroscopic studies (Scheme S3) (Figures S49−S54). UV thermal melting experiments were repeated with the $GCGT_6CGC$ heterooligomer (D10) and its complementary sequence (D13) (Table 4). The T_m for the D10•D13 control was 50.0 °C (Table S3). An insignificant change in T_m (−0.9 °C) was observed when the $GCGT_6CGC$ heterooligomer with 5′ hexynyl modification (D9) was used, suggesting that the alkyne unit alone does not largely influence stability of this duplex (Figure 5A). Interestingly, the DPA 104 conjugated ODN (D12) also had little effect on duplex stability. The D12 conjugate afforded ∼1.0 °C thermal stabilization when hybridized with D13 compared to the D10•D13 control (Table S3). A similar T_m change (+1.2 °C) was observed with hybridization of D12 to its complement RNA sequence (R5) as compared to the D10•R5 control (Table S4). Thus, we concluded that the 9 atom linker of DPA 104 was not optimal for the benzimidazole derivative to recognize the mixed base sequence.

UV thermal denaturation experiments were repeated with DPA 6011 conjugated ODN (D11, Figure 5A). Gratifyingly, a 5.0 °C increase in T_m was observed for the D11•D13 duplex versus the D10•D13 control (Table S3). Control experiments in which the D10•D13 duplex was denatured in the presence of increasing concentrations of unconjugated DPA 6011 (1 to 6 μM) resulted in no significant change in its T_m (−0.7 to +2.4 °C) (Figure S55, Table S5). These results suggest that an extended linker is needed for optimal recognition as it likely positions the benzimidazole moiety near the AT-rich stretch.

Fluorescence spectroscopy was used to monitor binding of the benzimidazole derivative through a fluorescence intensity

https://doi.org/10.1021/acsbiomedchemau.3c00074
ACS Bio Med Chem Au 2024, 4, 154−164

Table 4. 12 Mer Heterooligomer and Mismatch Sequences Used in this Study

Sequence	Code
5'-HexynylGCG TTT TTT CGC	D9
5'-d(GCG TTT TTT CGC)	D10
5'-d(GCG TTT TTT CGC)-DPA 6011	D11
5'-d(GCG TTT TTT CGC)-DPA 105	D12
5'-d(GCG AAA AAA CGC)	D13
5'-d(GCG AAA ACA CGC)	D14[a]
5'-d(GCG AAA ATA CGC)	D15[a]
5'-d(GCG AAA AGA CGC)	D16[a]
5'-d(GCG AAC AAA CGC)	D17[b]
5'-d(GCG AAT AAA CGC)	D18[b]
5'-d(GCG AAG AAA CGC)	D19[b]
5'-d(GCG CAA AAA CGC)	D20[c]
5'-d(GCG TAA AAA CGC)	D21[c]
5'-d(GCG GAA AAA CGC)	D22[c]
5'-r(GCG AAA AAA CGC)	R5

[a]Sequences D14-D16 contain an A to C, A to T, and A to G mismatch in the eighth position from 5′-end, respectively. [b]Sequences D17-D19 contain an A to C, A to T, and A to G mismatch in the sixth position from 5′-end, respectively. [c]Sequences D20-D22 contain an A to C, A to T, and A to G mismatch in the fourth position from 5′-end, respectively.

change. In the absence of a DNA duplex, the fluorescence of the benzimidazole derivative is low, with little change observed when heated (Figures S56 and S57). Upon titration of the complementary strand (D13), the fluorescence of DPA 6011 conjugated to ODN D11 increased and displayed a blue shift, indicating binding of the benzimidazole derivative to the duplex (Figure S58). Using CD spectroscopy, we found that the D11•D13 duplex maintains a B-form structure (Figure S59). Similar to complementary DNA duplexes formed with D2-D4, no CD signal was observed at ∼325 nm which would correspond to the benzimidazole moiety. We attribute the lack of the CD signal at ∼325 nm to be due to very weak absorption of the benzimidazole moiety at low duplex concentrations (≤4 μM). At higher duplex concentrations (∼36 μM), a positive peak at ∼325 nm was observed, which coincided with a weak absorption band for the benzimidazole moiety (Figure S60).

Sequence-specific recognition of the ODN-DPA 6011 conjugate was assessed by measuring its melting temperature upon hybridization to its RNA complement and mismatching DNA sequences. Hybridization of D11 with its RNA complement (R5) resulted in no change in thermal stabilization as compared to the D10•R5 control (Figure 5B). For mismatch DNA sequences, an adenine in D10 was replaced with cytosine (D14, D17 and D20), thymine (D15, D18 and D21), or guanine (D16, D19 and D22) to yield nine

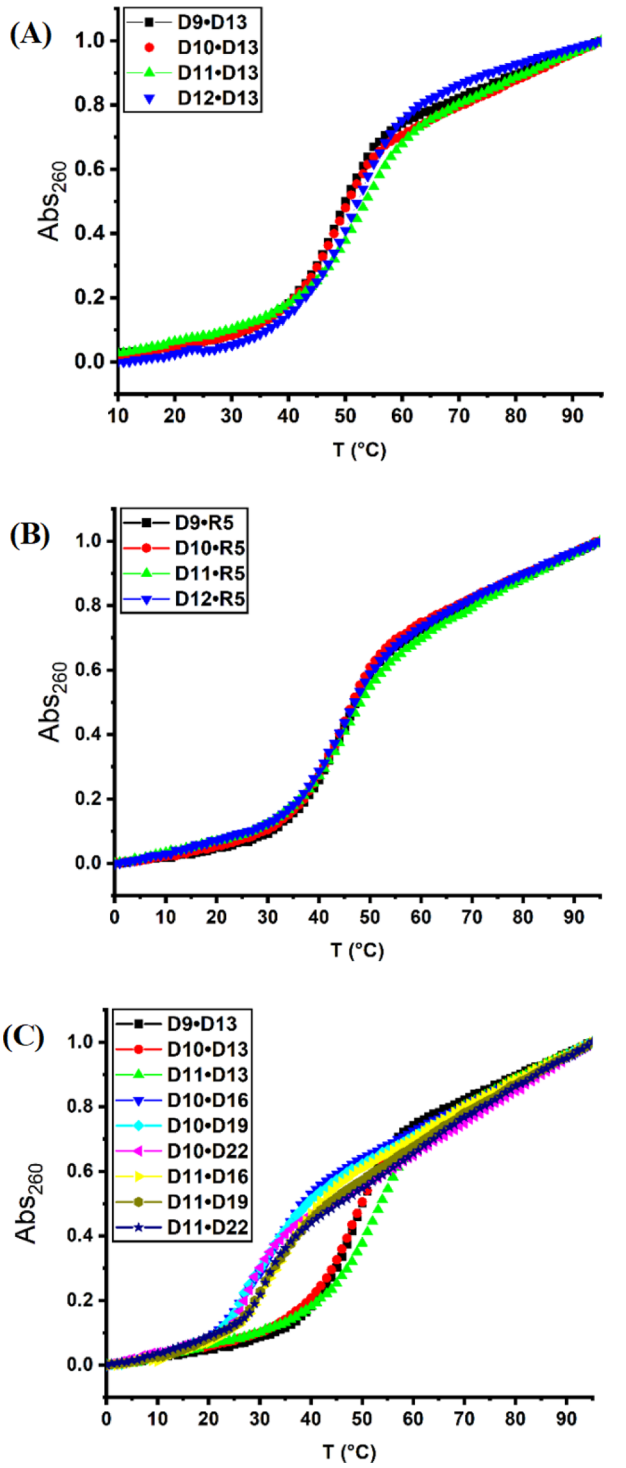

Figure 5. UV melting curves of DNA duplexes and DNA•RNA hybrids; (A) thermal denaturation profiles of DNA duplexes; (B) thermal denaturation profiles of DNA:RNA hybrids; (C) thermal denaturation profiles of DNA G-mismatch sequences with D10 and D11.

different DNA sequences (Table 4). A large decrease in T_m (11.9 to 25.0 °C) was observed for all mismatch DNA sequences hybridized to the nonbenzimidazole control DNA D10 as compared to the complementary D10•D13 duplex (Figure 5C). The extent of thermal destabilization was sequence dependent, as the largest decreases in T_m were observed with the A to T mismatch (−18.7 to −25.0 °C),

https://doi.org/10.1021/acsbiomedchemau.3c00074
ACS Bio Med Chem Au 2024, 4, 154−164

followed by A to G (−16.5 to −22.9 °C), and then A to C (−11.9 to −18.0 °C) (Table S3). Replacement of D10 with the D11 conjugate of the ODN-DPA 6011 further decreased the thermal stability of all mismatched DNA duplexes (Figure 5C). Indeed, the T_ms were 0.5 to 8.2 °C lower than those determined using the unconjugated D10 control (Table S3). Altogether, these results corroborate our findings that covalent conjugation of benzimidazoles to the ODN: (i) leads to stronger and preferential stabilization of DNA duplexes over unconjugated controls and DNA•RNA hybrids, (ii) enhances its sequence specificity, and (iii) does not significantly alter secondary structure upon binding ssDNA.

CONCLUSIONS

In this study, we evaluated the molecular recognition of ODNs that were post synthetically modified with a fluorescent benzimidazole moiety. By attaching a known DNA-binding ligand such as benzimidazole, we hypothesized that the stability and sequence specificity of the ODN would be enhanced upon hybridization with complementary sequences. Using click chemistry, we developed a general and efficient method to quickly synthesize five ODN-benzimidazole conjugates. This method uses Cu wire as the catalyst, which simplified metal removal post conjugation and avoided the use of reductant mixtures that can degrade the ODN.[34]

UV and fluorescence monitored thermal denaturation studies with hybridized ODN-benzimidazole conjugates provided valuable insights into the impact of covalent conjugation. ODN-benzimidazole conjugates hybridized to complementary ssDNA adopted B-form duplexes that had increased thermal stability as compared to unconjugated controls (ΔT_m = +5.0 to +12.0 °C). The increase in the thermal stability of these DNA duplexes is due to binding of the benzimidazole moiety, which is known to interact with the minor groove.[14−16] In addition to increased thermal stability, covalent conjugation of benzimidazoles to ODNs also enhanced sequence specificity. ODN-benzimidazole conjugates were found to preferentially stabilize complementary ssDNA (ΔT_m = +5.0 to +12.0 °C) over ssRNA (ΔT_m = 0.0 to +3.0 °C). Furthermore, thermal denaturation studies with a single base pair mismatch revealed larger destabilization for DNA duplexes that were hybridized to ODN-benzimidazole conjugates as compared to unconjugated controls ($\Delta\Delta T_m$ = −0.5 to −13.6 °C).

Molecular modeling studies with covalently attached ODN-benzimidazole DNA complexes illustrated how the benzimidazole moiety may bind the minor groove and how the length of the linker between the benzimidazole and azide moieties can affect binding. Indeed, a linker length dependence was observed with benzimidazoles conjugated to a dT_{15} homo-oligomer where the longest linker (D4) yielded the largest increase in thermal stability (ΔT_m = +12.0 °C) and also was most optimally placed in the minor groove. Furthermore, a different length linker was needed to enhance the thermal stability of a benzimidazole conjugated to a dT_6 heteroligomer, highlighting the importance of the linker in the design of the ODN-benzimidazole conjugates. A thorough investigation of the noncovalent interactions that may form between linkers and DNA duplexes could provide guiding principles for linker selection, but are outside the scope of this present work. Further biophysical and structural studies that evaluate the influence of linker length, composition, and placement on the hybridization of conjugates to ssDNA of varying lengths and sequences will yield fundamental insights into the design of conjugated ODN probes and diagnostics.

METHODS

All chemicals and solvents were of laboratory grade, as obtained from commercial suppliers, and were used without further purification.

Nucleic Acids

DNA and RNA oligomers were purchased from Integrated DNA Technologies (IDT) unless otherwise specified. Concentration of each oligomer was determined by UV absorbance at 260 nm using extinction coefficients provided by IDT: D1 and D1B = 122,100 ($M^{-1}cm^{-1}$), D5 = 183,400 ($M^{-1}cm^{-1}$), D6-D8 = 182,700 ($M^{-1}cm^{-1}$), R1 = 183,400 ($M^{-1}cm^{-1}$), R2-R4 = 182,700 ($M^{-1}cm^{-1}$), D9 and D10 = 101,400 ($M^{-1}cm^{-1}$), D13 = 124,200 ($M^{-1}cm^{-1}$), D14/D17/D20 = 119,800 ($M^{-1}cm^{-1}$), D15/D18/D21 = 122,300 ($M^{-1}cm^{-1}$), D16/D19/D22 = 123,500 ($M^{-1}cm^{-1}$), R5 = 123,600 ($M^{-1}cm^{-1}$). Concentration of each ODN-benzimidazole conjugate was determined by UV absorbance at 260 nm using extinction coefficients: 122,100 (M^{-1} cm^{-1}) (D2-D4) and 101,400 ($M^{-1}cm^{-1}$) (D11 and D12). DNA duplexes and DNA•RNA hybrids used for all experiments were preformed by heating strands at 95 °C for 5 min, then slowly annealing to room temperature, and storing at 4 °C for at least 12 h.

Synthesis of Azide Functionalized Benzimidazoles

Synthesis and characterization of DPA 102, 103, and 105 have been reported elsewhere.[35−37] Synthetic procedures and characterization for DPA 104 and 6011 are listed in the Supporting Information.

Conjugation of Benzimidazoles to ssDNA

An azide functionalized benzimidazole (DPA 102−105 or DPA 6011) was dissolved to 0.10 M in 1:1 dimethyl sulfoxide:methanol. The 15 mer or 9 mer 5′-hexynyl modified DNA (D1 or D9) was dissolved to 1.0 mM in H_2O. Solutions of azide functionalized benzimidazole and hexynyl modified DNA were combined so that the final concentrations were 14 and 0.72 mM, respectively. Additionally, copper wire was added as the catalyst, and the reaction was stirred at room temperature for up to 22 h. Conjugated products D2-D4 were directly purified by reverse phase HPLC to afford analytically pure samples by eluting with a linear gradient of 0 to 20% acetonitrile (ACN) in 0.10 M triethylammonium acetate buffer (pH 7.0) over 30 min. The column used in the purification was a LiChrospher 100-RP 18 column (5 μm). Conjugated products D11 and D12 were directly purified by using Biospin columns with Bio-Gel P6 (BioRad) to afford analytically pure samples.

Purified conjugates were analyzed by Matrix Assisted Laser Desorption Ionization-Time of Flight (MALDI-TOF) mass spectrometry using a Bruker Microflex mass spectrometer in reflector negative mode. The dried droplet method was used to prepare the samples. Specifically, samples were prepared by mixing 3-hydroxypicolinic acid (25 mg/mL) and the conjugate in 1:1 acetonitrile/water. For conjugates D11 and D12, ammonium citrate dibasic was also included (2.5 mg/mL).

Additionally, purified conjugates were analyzed by ultrahigh performance liquid chromatography mass spectrometry (UPLC-MS) using a Waters SQD2 with H-class UPLC. The column used was an Acquity Premier Oligonucleotide BEH C18 (1.7 μm). Mobile phase: A) 90% H_2O, 10% MeOH, 15 mM TEA, 25 mM HFIP; B) 90% MeOH, 10% H_2O. Method: 100% A for 2 min, 0−70% B over 2 min, 70−95% B over 1 min, 95−5% B over 2 min, 5% B for 1 min. Flow rate: 0.3 mL/min. PDA at 254 nm.

Thermal Denaturation Monitored by Ultraviolet (UV) Spectroscopy

Solutions containing preformed nucleic acid duplexes (1.0 or 2.0 μM/strand) in 10 mM sodium cacodylate, 0.50 mM EDTA, and 0.10 M NaCl (pH 7.0) were prepared. UV thermal denaturation experiments were performed on an Agilent Cary 300 spectrophotometer equipped with a multicell Peltier controlled cell holder. Prior to heating, samples were equilibrated at 0 or 10 °C for 30 min. Then, samples

https://doi.org/10.1021/acsbiomedchemau.3c00074
ACS Bio Med Chem Au 2024, 4, 154−164

were heated from 10 to 80 or 95 °C and the data collection was recorded in 0.25 or 1.0 °C steps by monitoring absorbance at 260 nm. The thermal denaturation profiles were plotted using Origin 5.0 or Pro2023 software. Thermal melting (T_m) values were determined from first-order derivatives.

Circular Dichroism (CD) Spectroscopy

CD was performed using a Jasco J-810 CD spectropolarimeter equipped with a Peltier temperature controller and a 1.0 cm quartz cuvette. Solutions contained preformed DNA duplexes and DNA•RNA hybrids (4.0 or 1.0 μM/duplex) in 10 mM sodium cacodylate, 0.50 mM EDTA, and 0.10 M NaCl (pH 7.0). Spectra of preformed DNA duplexes and DNA•RNA hybrids were obtained at 10 or 20 °C with data collection at a rate of either 50 or 200 nm/min.

Thermal Denaturation Monitored by Fluorescence Spectroscopy

Solutions containing preformed nucleic acid duplexes (1.0 μM/strand) in 10 mM sodium cacodylate, 0.50 mM EDTA and 0.10 M NaCl (pH 7.0) were prepared. All measurements were made on a Photon Technology QuantaMaster fluorometer (PTI) equipped with a temperature controller (Quantum Northwest) and a Coherent T255P water chiller (ThermoTek). Emission was measured from 380 or 400 to ∼600 nm with an excitation wavelength of 340 or 350 and 1 nm slit widths. The fluorescence was measured at every 10 °C increase from 20 to 90 °C in 5.5 nm steps. T_m values were determined using the method reported by Mergny, J-L and Lacroix, L.[38] Upper and lower baselines were drawn, corresponding to the unfolded and folded forms, respectively. Then, a median line was drawn between the two baselines. The crossing point between the experimental curve and the median is the T_m.

Molecular Modeling

Discovery Studio was employed to prepare models of DNA-benzimidazole conjuates hybridized to its complementary sequence.[39] Autodock4 was used for molecular docking of unconjugated benzimidazoles with complementary DNA duplexes.[40] The duplexes were prepared for molecular docking simulation by adding hydrogen atoms and the subsequent addition of Kollman charges. Coordinates of each compound were generated using ChemDraw15.0, followed by MM2 energy minimization. The binding pocket for Autodock4 was defined by a grid box. The grid box was created with 60 points equally in each direction of x, y, and z. AutoGrid4 was used to produce grid maps for AutoDock4 calculations where the search space size utilized grid points of 0.375 Å. The Lamarckian genetic algorithm was opted to search for the best conformers. Final docked conformations were clustered using a tolerance of 1.00 root-mean-square deviation. The best model was picked based on the most negative stabilization energy. Models were visualized using Chimera.[41] The energy calculations were carried out using Argus lab, and Hamiltonian Quantum mechanical calculation was done using the Hartree−Fock SCF theorem considering maximum iterations value of 200 kcal mol^{-1}.[42]

■ ASSOCIATED CONTENT

Supporting Information

The Supporting Information is available free of charge at https://pubs.acs.org/doi/10.1021/acsbiomedchemau.3c00074.

UPLC-MS profiles, UV scans, fluorescence scans, thermal denaturation profiles, circular dichroism plots, MALDI-TOF spectra, and docking structures of benzimidazole-oligodeoxynucleotide conjugates (PDF)

■ AUTHOR INFORMATION

Corresponding Author

Dev P. Arya − *Laboratory of Medicinal Chemistry, Department of Chemistry, Clemson University, Clemson, South Carolina 29634, United States;* orcid.org/0000-0001-5873-1066; Email: dparya@clemson.edu

Authors

Souvik Sur − *Laboratory of Medicinal Chemistry, Department of Chemistry, Clemson University, Clemson, South Carolina 29634, United States*

Suresh Pujari − *Laboratory of Medicinal Chemistry, Department of Chemistry, Clemson University, Clemson, South Carolina 29634, United States*

Nihar Ranjan − *Laboratory of Medicinal Chemistry, Department of Chemistry, Clemson University, Clemson, South Carolina 29634, United States;* orcid.org/0000-0003-3581-4605

Lidivine Azankia Temgoua − *Laboratory of Medicinal Chemistry, Department of Chemistry, Clemson University, Clemson, South Carolina 29634, United States*

Sarah L. Wicks − *Laboratory of Medicinal Chemistry, Department of Chemistry, Clemson University, Clemson, South Carolina 29634, United States;* orcid.org/0000-0002-8068-5462

Andrea Conner − *Laboratory of Medicinal Chemistry, Department of Chemistry, Clemson University, Clemson, South Carolina 29634, United States*

Complete contact information is available at: https://pubs.acs.org/10.1021/acsbiomedchemau.3c00074

Author Contributions

CRediT: **Souvik Sur** data curation, writing-review & editing; **Suresh Pujari** data curation, writing-original draft; **Nihar Ranjan** data curation; **Lidivine Azankia Temgoua** data curation; **Sarah L. Wicks** data curation, writing-review & editing; **Andrea Conner** data curation, investigation, writing-review & editing; **Dev Priya Arya** conceptualization, formal analysis, funding acquisition, methodology, project administration, supervision, writing-review & editing.

Notes

The authors declare no competing financial interest.

■ ACKNOWLEDGMENTS

We thank the National Institutes of Health for financial support (grants R42GM097917, AI114114) to D.P.A.

■ ABBREVIATIONS

ODN	oligodeoxynucleotide
ss	single stranded
ds	double stranded
MALDI-TOF	matrix assisted laser desorption ionization-time-of-flight
UPLC-MS	ultrahigh performance liquid chromatography mass spectrometry
UV−vis	ultraviolet−visible
Tm	thermal melting temperature
CD	circular dichroism
IDT	integrated DNA technologies
ACN	acetonitrile

■ REFERENCES

(1) Toulme, J. J.; Krisch, H. M.; Loreau, N.; Thuong, N. T.; Helene, C. Specific Inhibition of mRNA Translation by Complementary Oligonucleotides Covalently Linked to Intercalating Agents. *Proc. Natl. Acad. Sci. U. S. A.* **1986**, *83*, 1227−1231.

(2) Milne, L.; Xu, Y.; Perrin, D. M.; Sigman, D. S. An Approach to Gene-Specific Transcription Inhibition Using Oligonucleotides Complementary to the Template Strand of the Open Complex. *Proc. Natl. Acad. Sci. U. S. A.* **2000**, *97*, 3136−3141.
(3) Dias, N.; Stein, C. A. Antisense Oligonucleotides: Basic Concepts and Mechanisms. *Mol. Cancer Ther.* **2002**, *1*, 347−355.
(4) Egli, M.; Manoharan, M. Chemistry Structure and Function of Approved Oligonucleotide Therapeutics. *Nucleic Acids Res.* **2023**, *51*, 2529−2573.
(5) Wiederholt, K.; Rajur, S. B.; Giuliano, J.; O'Donnel, M. J.; McLaughlin, L. W. DNA-Tethered Hoechst Groove-Binding Agents: Duplex Stabilization and Fluorescence Characteristics. *J. Am. Chem. Soc.* **1996**, *118*, 7055−7062.
(6) Bethge, L.; Jarikote, D. V.; Seitz, O. New Cyanine Dyes as Base Surrogates in PNA: Forced Intercalation Probes (FIT-probes) for Homogeneous SNP Detection. *Bioorg. Med. Chem.* **2008**, *16*, 114−125.
(7) Danielsen, M. B.; Christensen, N. J.; Jørgensen, P. T.; Jensen, K. J.; Wengel, J.; Lou, C. Polyamine-functionalized 2'-amino-LNA in Oligonucleotides: Facile Synthesis of New Monomers and High-Affinity Binding Towards ssDNA and dsDNA. *Chem. - Eur. J.* **2021**, *27*, 1416−1422.
(8) Franzini, R. M.; Kool, E. T. Efficient Nucleic Acid Detection by Templated Reductive Quencher Release. *J. Am. Chem. Soc.* **2009**, *131*, 16021−16023.
(9) Hwang, G. T. Single-Labeled Oligonucleotides Showing Fluorescence Changes Upon Hybridization with Target Nucleic Acids. *Molecules* **2018**, *23*, 124.
(10) Krasheninina, O. A.; Novopashina, D. S.; Apartsin, E. K.; Venyaminova, A. G. Recent Advances in Nucleic Acid Targeting Probes and Supramolecular Constructs Based on Pyrene-Modified Oligonucleotides. *Molecules* **2017**, *22*, 2108.
(11) Hawner, M.; Ducho, C. Cellular Targeting of Oligonucleotides by Conjugation with Small Molecules. *Molecules* **2020**, *25*, 5963.
(12) Kar, S. S.; Dhar, A. K.; Palei, N. N.; Bhatt, S. Small-Molecule Oligonucleotides as Smart Modality for Antiviral Therapy: A Medicinal Chemistry Perspective. *Future Med. Chem.* **2023**, *15*, 1091−1110.
(13) Winkler, J. Oligonucleotide Conjugates for Therapeutic Applications. *Ther. Delivery* **2013**, *4*, 791−809.
(14) Harshman, K. D.; Dervan, P. B. Molecular Recognition of B-DNA by Hoechst 33258. *Nucleic Acids Res.* **1985**, *13*, 4825−4835.
(15) Abu-Daya, A.; Brown, P. M.; Fox, K. R. DNA Sequence Preferences of Several AT-Selective Minor Groove Binding Ligands. *Nucleic Acids Res.* **1995**, *23*, 3385−3392.
(16) Bucevicius, J.; Lukinavicius, G.; Gerasimaite, R. The Use of Hoechst Dyes for DNA Staining and Beyond. *Chemosensors* **2018**, *6*, 18.
(17) Pjura, P. E.; Grzeskowiak, K.; Dickerson, R. E. Binding of Hoechst 33258 to the Minor Groove of B-DNA. *J. Mol. Biol.* **1987**, *197*, 257−271.
(18) Teng, M. K.; Usman, N.; Frederick, C. A.; Wang, A. H. The Molecular Structure of the Complex of Hoechst 33258 and the DNA Dodecamer d(CGCGAATTCGCG). *Nucleic Acids Res.* **1988**, *16*, 2671−2690.
(19) Wiederholt, K.; Rajur, S. B.; McLaughlin, L. W. Oligonucleotides Tethering Hoechst 33258 Derivatives: Effect of the Conjugation Site on Duplex Stabilization and Fluorescence Properties. *Bioconjugate Chem.* **1997**, *8*, 119−126.
(20) Hegde, M.; Kumar, K. S. S.; Thomas, E.; Ananda, H.; Raghavan, S. C.; Rangappa, K. S. A Novel Benzimidazole Derivative Binds to the DNA Minor Groove and Induces Apoptosis in Leukemic Cells. *RSC Adv.* **2015**, *5*, 93194−93208.
(21) Miao, Y.; Lee, M. P. H.; Parkinson, G. N.; Batista-Parra, A.; Ismail, M. A.; Neidle, S.; Boykin, D. W.; Wilson, W. D. Out-of-shape DNA Minor Groove Binders: Induced Fit Interactions of Heterocyclic Dications with the DNA Minor Groove. *Biochemistry* **2005**, *44*, 14701−14708.
(22) Ebenezer, O.; Oyetunde-Joshua, F.; Omotoso, O. D.; Shapi, M. Benzimidazole and its Derivatives: Recent Advances (2020−2022). *Results Chem.* **2023**, *5*, 100925.
(23) Farahat, A. A.; Bennett-Vaughn, C.; Mineva, E. M.; Kumar, A.; Wenzler, T.; Brun, R.; Liu, Y.; Wilson, W. D.; Boykin, D. W. Synthesis, DNA Binding and Antitrypanosomal Activity of Benzimidazole Analogues of DAPI. *Bioorg. Med. Chem. Lett.* **2016**, *26*, 5907−5910.
(24) Chen, C.; Li, X.; Zhao, H.; Liu, M.; Du, J.; Zhang, J.; Yang, X.; Hou, X.; Fang, H. Discovery of DNA-Targeting HDAC Inhibitors with Potent Antitumor Efficacy In Vivo that Trigger Antitumor Immunity. *J. Med. Chem.* **2022**, *65*, 3667−3683.
(25) Rostovtsev, V. V.; Green, L. G.; Fokin, V. V.; Sharpless, K. B. A Stepwise Huisgen Cycloaddition Process: Copper(I)-Catalyzed Regioselective "Ligation" of Azides and Terminal Alkynes. *Angew. Chem., Int. Ed.* **2002**, *41*, 2596−2599.
(26) Meldal, M.; Tornoe, C. W. Cu-Catalyzed Azide-Alkyne Cycloaddition. *Chem. Rev.* **2008**, *108*, 2952−3015.
(27) Dumousseau, M.; Rodriguez, N.; Juty, N.; Le Novere, N. MELTING, a Flexible Platform to Predict the Melting Temperatures of Nucleic Acids. *BMC Bioinf.* **2012**, *13*, 101.
(28) Le Novere, N. MELTING, computing the melting temperature of nucleic acid duplex. *Bioinformatics* **2001**, *17*, 1226−1227.
(29) Wiederholt, K.; McLaughlin, L. W. Duplex Stabilization by DNA-Hoechst 33258 Conjugates: Effects of Base Pair Mismatches. *Nucleosides Nucleotides* **1998**, *17*, 1895−1904.
(30) Salazar, M.; Fedoroff, O. Y.; Miller, J. M.; Ribeiro, N. S.; Reid, B. R. The DNA Strand in DNA.RNA Hybrid Duplexes is Neither B-form nor A-form in Solution. *Biochemistry* **1993**, *32*, 4207−4215.
(31) Watson, J. D.; Crick, F. H. C. Molecular Structure of Nucleic Acids: A Structure for Deoxyribose Nucleic Acid. *Nature* **1953**, *171*, 737−738.
(32) Willis, B.; Arya, D. P. Recognition of RNA Duplex by a Neomycin-Hoechst 33258 Conjugate. *Bioorg. Med. Chem.* **2014**, *22*, 2327−2332.
(33) Hung, S. H.; Yu, Q.; Gray, D. M.; Ratliff, R. L. Evidence from CD Spectra that d(purine).r(pyrimidine) and r(purine).d(pyrimidine) Hybrids are in Different Structural Classes. *Nucleic Acids Res.* **1994**, *22*, 4326−4334.
(34) Liu, P. Y.; Jiang, N.; Zhang, J.; Wei, X.; Lin, H. H.; Yu, X. Q. The Oxidative Damage of Plasmid DNA by Ascorbic Acid Derivatives In Vitro: The First Research on the Relationship Between the Structure of Ascorbic Acid and the Oxidative Damage of Plasmid DNA. *Chem. Biodiversity* **2006**, *3*, 958−966.
(35) Ranjan, N.; Story, S.; Fulcrand, G.; Leng, F.; Ahmad, M.; King, A.; Sur, S.; Wang, W.; Tse-Dinh, Y.; Arya, D. Selective Inhibition of *Escherichia coli* RNA and DNA Topoisomerase I by Hoechst 33258 Derived Mono- and Bisbenzimidazoles. *J. Med. Chem.* **2017**, *60*, 4904−4922.
(36) Ranjan, N.. Targeting Duplex and Higher Order Nucleic Acids Using Neomycin/Neomycin-Hoechst 3325 8 Conjugates,In *Ph.D. Dissertation*: Clemson University; Clemson, SC, 2017. https://tigerprints.clemson.edu/all_dissertations/1937. (accessed 2024−01−02).
(37) Nahar, S.; Ranjan, N.; Ray, A.; Arya, D. P.; Maiti, S. Potent Inhibition of miR-27a by Neomycin-Bisbenzimidazole Conjugates. *Chem. Sci.* **2015**, *6*, 5837−5846.
(38) Mergny, J.-L.; Lacroix, L. Analysis of Thermal Melting Curves. *Oligonucleotides* **2003**, *13*, 515−537.
(39) *Dassault Systemes Release Version 3.0: BIOVIA Discovery Studio; Dassault Systemes: France*, 2010.https://www.3ds.com/products/biovia/discovery-studio. (accessed 2018−03−26).
(40) Trott, O.; Olson, A. J. AutoDock Vina: Improving the Speed and Accuracy of Docking with a New Scoring Function, Efficient Optimization, and Multithreading. *J. Comput. Chem.* **2010**, *31*, 455−461.
(41) Pettersen, E. F.; Goddard, T. D.; Huang, C. C.; Couch, G. S.; Greenblatt, D. M.; Meng, E. C.; Ferrin, T. E. UCSF Chimera—A

Visualization System for Exploratory Research and Analysis. *J. Comput. Chem.* **2004**, *25*, 1605−1612.
(42) *Planaria Software Release 4.0.1: ArgusLab; Planaria Software*, LLC: Washington, 2004.http://www.arguslab.com/arguslab.com/ArgusLab.html. (accessed 2018−03−26).

https://doi.org/10.1021/acsbiomedchemau.3c00074
ACS Bio Med Chem Au 2024, 4, 154−164